Results in Chemistry 13 (2025) 101975

Contents lists available at ScienceDirect

Results in Chemistry

journal homepage: www.sciencedirect.com/journal/results-in-chemistry

Using of multi-phase thermal model of the lattice Boltzmann method for simulation of two-phase Rayleigh–Bénard convective heat transfer

Murtadha M. Al-Zahiwat [a], Ihab Omar [b], Shahram Babadoust [c], Laith S. Sabri [d], Arian Yazdkhsti [e], S. Mohammad Sajadi [f], Abbas Deriszadeh [g], Nafiseh Emami [h,*]

[a] Department of Chemical engineering, College of Engineering, University of Misan, Amarah, Iraq
[b] Air Conditioning Engineering Department, Faculty of Engineering, Warith Al-Anbiyaa University, Karbala 56001, Iraq
[c] Department of Medical Biochemical Analysis, Cihan University-Erbil, Erbil, Kurdistan Region, Iraq
[d] Department of Chemical Engineering, University of Technology- Iraq, Baghdad, Iraq
[e] Department of Mechanical Engineering, Isfahan University of Technology, Isfahan 84156-83111, Iran
[f] Department of Chemistry, Payam e Noor University, Saqqez Branch, Saqqez, Kurdistan, Iran
[g] Department of Chemical Engineering, University of Sistan and Baluchestan, Zahedan, Iran
[h] Department of Chemical Engineering, Faculty of Engineering, Isfahan university, Iran

ARTICLE INFO

Keywords:
Multi-phase thermal flow
Lattice Boltzmann method
Rayleigh–Bénard

ABSTRACT

In this study, the neutral scalar thermal model is presented for single-phase and so, a single-phase Rayleigh–Bénard is investigated. The Shan-Chen model is expressed in the isothermal state, and by combining the two models, the mixed Shan-Chen thermal method is presented. Then, using a mixed model, a two-phase Rayleigh–Bénard with the thermal Shan-Chen method is proposed. Two-phase Rayleigh–Bénard convective heat transfer is simulated at the relatively high Rayleigh numbers (10^5), different Capillary numbers (10^{-3} to 10^{-4}), and also, various ε parameters (parameters related to the temperature difference and thermal expansion). In two-phase Rayleigh–Bénard convective heat transfer increasing the Rayleigh number leads to the increment of Rayleigh–Bénard convective heat transfer between the hot and cold wall and the temperature gradient enhances in the vicinity of the upper wall, lower wall, and interface. It is worth mentioning, that in the two-phase Rayleigh–Bénard problem, the variations of the interface are changed only by changing the thermal expansion coefficient and the temperature difference between the two walls. The results show that the mixed model can simulate two-phase thermal flows. The stability of this method is the same as the multi-phase isothermal models, and it can be applied well for different state equations and relatively high Rayleigh numbers.

Introduction

One of the challenges in simulating multi-phase systems by using the computational fluid dynamic (CFD) is the method for detecting the location of the interface and applying appropriate boundary conditions at that location. Hence, in the last years, the Lattice Boltzmann Method was proposed for modeling these flows. In multi-phase problems, automatic detection of the location of the interface, the feasibility of parallel processing, and low computational cost lead to this method, especially in multi-phase problems. Due to the observation of multi-phase flows in most industrial and natural processes, researchers have investigated these kinds of flows experimentally and theoretically. In recent years, many studies have been conducted on multiphase flows. However, multiphase thermal flows have not been studied enough. Rayleigh– Bénard convection is the coordinated movement of a fluid that is confined between two thermally conducting plates and is heated from below to produce a temperature difference. An uncoordinated movement of fluid particles which allows energy transfer between lower and upper plates is substituted by a coordinated movement above a certain temperature gradient. One of the most common multi-phase thermal problems is two-phase Rayleigh–Bénard convective heat transfer. The implemented works in the field of LBM for multi-phase thermal problems are so limited. The research of He et al. [1] and Zhan and Chen [2] can be mentioned as the earliest studies. They presented a model of the Shan-Chen method of LBM which is capable of simulating multi-phase thermodynamic flows. This method is stable from the thermodynamic perspective at the macroscopic scale. For the

* Corresponding author.
E-mail addresses: nafise.emami@iaukhsh.ac.ir, nafisehemami6672@gmail.com (N. Emami).

https://doi.org/10.1016/j.rechem.2024.101975
Received 7 September 2024; Accepted 12 December 2024
Available online 14 December 2024

Nomenclature

A	Acceleration of channel (m/s^2)
Ca	Capillary number
c_s	Lattice Sound speed (m/s)
e_α	Lattice particle Microscopic velocity along α direction (m/s)
F	Particles' interaction force (N)
f_α	The distribution function for flow
f^{eq1}	The equilibrium distribution function for the flow domain
G	The intensity of fluid/fluid interaction
g	Gravitational acceleration
g_α	The distribution function for the temperature domain
g^{eq}	The equilibrium distribution function for the temperature domain
Nu	Nusselt number
N	Grid size
P	Pressure
R	Particle Radius (m)
Ra	Rayleigh number
T	Temperature (K)
T^*	Reference temperature (K)
u	Macroscopic velocity vector in x-direction (m/s)
u^{eq}	Equilibrium velocity (m/s)
u,v	Horizontal and vertical components of velocity (m/s)
L	The length of the horizontal wall
h	The distance between the peak and the valley in an interface wave
x	The length of the x-direction

Greek symbols

κ	Thermal dissipation coefficient (m^2/s)
β	Thermal expansion coefficient (K^{-1})
ρ	Density (kg/m^3)
ψ	Effective mass
ω_α	Weight coefficient along α-direction
τ_v	The relaxation time of the flow domain
τ_T	The relaxation time of the temperature domain
μ	Dynamic viscosity (N.m/ s)
θ	Contact angle

Subscripts

i	Grid direction
ads	Solid-liquid
ave	Average
0	Reference

first time, by utilizing this model, generating liquid–vapor, boiling processes, and coagulation were simulated by proposing temperature as a neutral scalar. First, Yuan and Schaefer [3] described multi-phase relations of isothermal lattice Boltzmann. Then, they explained the neutral scalar model of lattice Boltzmann. They carried out a two-phase thermal lattice Boltzmann model by combining these two methods. The application of the new model was investigated by presenting numerical modeling results of a two-phase thermal system inside a rectangular-shaped channel. Chang and Alexander [4] improved a hybrid model of lattice Boltzmann for a two-phase fluid. So, they molded the temperature domain by applying the finite difference method and energy transfer equation. Their results show that the variations in the interface are due to the temperature difference and thermal expansion coefficient. Dong et al. [5] modeled the bubble growth and exit from the superheated surface by applying the hybrid thermal method of LBM and also, modified the multi-phase Shan-Chen model. Atter and Korner [6] studied developing an algorithm for using LBM to solve thermal free-surface flow with the liquid–solid phase changes. In addition, they utilized the free-energy model and neutral scalar method for simulating thermal flow and multi-phase flow, respectively. Chen et al. [7] performed a hybrid model of thermal lattice Boltzmann described boundary properties according to the total enthalpy. According to that the present methods are insufficient for thermal flow about the effect of interaction between the droplet and walls in multi-component problems. Ikeda [8] presented a new method that is capable of modeling multi-component multi-phase thermal lattice Boltzmann with high accuracy. Gong and Cheng [9] performed the bubble growth and exit from a superheated wall in the pool boiling by utilizing a new development model of the Shan-Chen model of LBM. Kamali et al. [10] investigated a numerical method for solving energy consistency equations in two phases when the effects of phase change are considered. Taghilou and Rahimian [11] used a thermal lattice Boltzmann method for modeling the behavior of a droplet on a solid wall. They utilized the free energy model [12] to obtain the results of the interaction between the droplet and the surface. The contact angle between the gas, liquid, and solid phases was applied in their work. Their numerical results indicated that by enhancing the

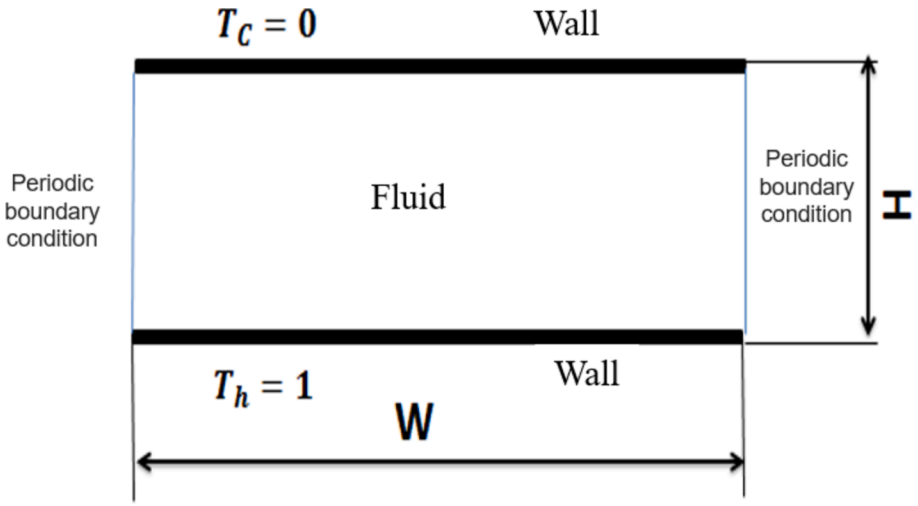

Fig. 1. Schematic view of single-phase Rayleigh–Bénard and its boundary conditions.

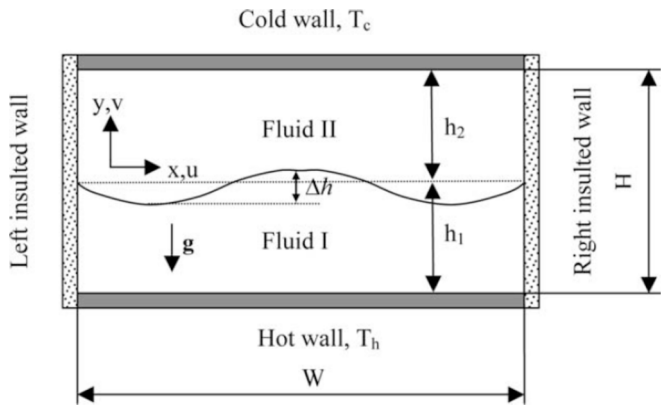

Fig. 2. Schematic graph of two-phase Rayleigh–Bénard and its related parameters.

ratio of the Prandtl number between the droplet and its surroundings, thermal dissipation will be delayed inside the droplet. This leads to a decrease in average droplet temperature. They represented that the heat flux is focused around the droplet. However, it is not considered in the gas phase. Li et al. [13] implemented a thermal hybrid model of LBM for modeling multi-phase thermal flows by applying a modified Shan-Chen model. TThe numerical results show that the fundamental heat transfer characteristics in the boiling such as strong transient heat flux fluctuations in the boiling transfer and the property that the maximum latent heat transfer coefficient in the superheat wall is lower than the maximum heat flux were presented as well in this method. In Ref. [13], phase change was investigated, while in the present research, Rayleigh-Bernard heat transfer was investigated. In addition, researchers [14–17] presented the influences of additives on the thermal behavior of convectional fluid and reported an increased heat transfer rate. Their results show that streamlining enhances with the rise of the Rayleigh number, while, it decreases with increasing Hartmann number and particle volume fraction. Multi-phase thermal LBM was studied in a limited way, however, in the present research; it is investigated by using the thermal Shan-Chen method for the first time. This method of heat transfer is simulated for the first time with the Shan-Chen two-phase model. The ability to simulate thermal two-phase problems with the Shan-Chen model is one of the innovations of this research. The results indicate that the mixed model is capable of simulating two-phase thermal flows.

Problem statement

Problem statement in the single-phase Rayleigh–Bénard simulation

Rayleigh–Bénard convective heat transfer is a good criterion for a thermal system in which a horizontal layer of fluid is heated from the bottom and the upper boundary is at a lower temperature. In Rayleigh–Bénard convective heat transfer when the temperature difference between upper and lower boundaries is too much, the static conduction becomes unstable. The temperature of the lower wall (y = 0) and upper wall (y = 1) are considered $T_h = 1$ and $T_c = 0$, respectively. The schematic view of Rayleigh–Bénard convective heat transfer and boundary conditions are presented in Fig. 1. According to this figure, the periodic boundary condition is applied to the left and right sides, while; the wall boundary condition is applied to up and downsides (horizontal walls). In this figure, H and W are the distance between two walls and the length of the wall, respectively.

Problem statement for Rayleigh–Bénard heat transfer in a two-phase system

Rayleigh–Bénard convective heat transfer is used extensively in the industry. Here, this problem is described by using LBM. In the previous section, this problem is presented as a single phase. Here, two immiscible fluids with different temperatures are proposed which are between two isothermal solid plates. Fig. 2 shows these two parallel plates and the interface of two fluids. The system is two layers of immiscible fluids with the same thickness of $h_1 = h_2 = 0.5H$, the width of W, and the height of H. The ratio of densities is $\rho_r = 0.33$. According to Fig. 2, the deformation of the interface is considered as $\varepsilon = \frac{\Delta h}{H}$. As mentioned, the lower wall is hot with a temperature of $T_h = 1$ and the upper wall is cold with a temperature of $T_c = 0$. In this figure, the vertical walls are considered periodic. At the beginning of the process, the interface is a straight line, which becomes a parabola by applying two Rayleigh–Bénard phases.

Governing equations in the thermal Shan-Chen method of LBM

Governing equations in multi-phase LBM

This method was invented by Shan and Chen [14] in 1993 and was called their names. Nowadays, among all multi-component or multi-phase lattice Boltzmann models, the Shan-Chen method has extensive application due to its high flexibility and simplicity. In the multi-phase multi-component Shan-Chen method of LBM, a distribution function is determined. The application of this method is in simulating the common surface of two-phase currents without calculating the surface tension. All multiphase and multicomponent fluids can be simulated with this method. The following equations are written for each distribution function [3]:

$$f_\alpha(x + e_\alpha \delta t,\ t + \delta t) = f_\alpha(x,t) - \frac{1}{\tau_\nu}[f_\alpha(x,t) - f_\alpha^{eq}(x,t)] \tag{1}$$

Where τ_ν is called the relaxation time for the flow field. f_α is distribution function for flow, In addition, in this model, the equilibrium distribution function is determined as [3]:

$$f_\alpha^{eq}(x,t) = \omega_\alpha \rho(x)[1 + \frac{3e_\alpha.u^{eq}}{c_s^2} + \frac{9(e_\alpha.u^{eq})^2}{2c_s^4} + \frac{3u^{eq\,2}}{2c_s^2}] \tag{2}$$

where ω_α, c_s and u^{eq} are the weight coefficient, sound speed in the grid unit, and equivalent velocity, respectively. In the D_2Q_9 model which is used in this research [3]:

$$e_{\alpha i} = \begin{bmatrix} 0 & 1 & 0 & -1 & 0 & 1 & -1 & -1 & 1 \\ 0 & 0 & 1 & 0 & -1 & 1 & 1 & -1 & 1 \end{bmatrix} \tag{3}$$

$$\omega_\alpha = [\frac{4}{9}\ \frac{1}{9}\ \frac{1}{9}\ \frac{1}{9}\ \frac{1}{36}\ \frac{1}{36}\ \frac{1}{36}\ \frac{1}{36}] \tag{4}$$

Macroscopic properties are computed as follows:

$$\rho = \sum_\alpha^N f_\alpha = \sum_\alpha^N f_\alpha^{eq} \tag{5}$$

$$\rho u = \sum_\alpha^N f_\alpha e_\alpha = \sum_\alpha^N f_\alpha^{eq} e_\alpha \tag{6}$$

Where ρ is the viscosity determined as:

$$\upsilon_\sigma = c_s^2(\tau_\sigma - 0.5\delta t) \tag{7}$$

The F is the interaction between particles which includes the intermolecular forces such as the volume forces, fluid–solid, and fluid–fluid forces. The interaction force of fluid–fluid at each point of the grid can be computed as follows:

$$\mathbf{F}_1(\mathbf{x},\mathbf{t}) = -\mathbf{G}(\mathbf{x})\left(\sum_{\alpha}\omega_{\mathbf{a}}\psi(\mathbf{x}+\mathbf{e}_{\alpha}\delta\mathbf{t},\mathbf{t})\mathbf{e}_{\alpha}\right) \tag{8}$$

In Equation (8), G is the intermolecular power parameter influencing the obtained results by using the Shan-Chen model from the numerical and physical perspective. ψ(x) is a molecular potential function. The molecular potential function of ψ(x) is expressed as the function of x by its dependency on the density and is called the effective mass [18]:

$$\boldsymbol{\psi}(\boldsymbol{x}) = \boldsymbol{\rho}_0[1 - \mathbf{exp}\left(-\frac{\boldsymbol{\rho}(\boldsymbol{x},\boldsymbol{t})}{\boldsymbol{\rho}_0}\right)] \tag{9}$$

Where constant of $\boldsymbol{\rho}_0$ is the reference density. By selecting the various shapes for ψ(x) in the above equation, it can be achieved different state equations for single-component multi-phase non-ideal fluid. Eventually, by using the effective weight function, the below state function is presented for computing pressure as follows:

$$\mathbf{p} = \mathbf{c}_s^2\boldsymbol{\rho} + \boldsymbol{c}_0\boldsymbol{G}[\boldsymbol{\psi}(\boldsymbol{x})]^2 \tag{10}$$

If the fluid is in the vicinity of the surface, a force is proposed for the interaction of fluid–solid:

$$\mathbf{F}_{\mathbf{ads}}(\boldsymbol{x},\boldsymbol{t}) = -\boldsymbol{G}_{\boldsymbol{ads}}\boldsymbol{\rho}(\boldsymbol{x},\boldsymbol{t})\sum_{\alpha}\omega_{\mathbf{a}}\mathbf{s}(\mathbf{x}+\mathbf{e}_{\alpha}\delta\mathbf{t})\mathbf{e}_{\alpha} \tag{11}$$

where $\boldsymbol{s}(\boldsymbol{x}+\boldsymbol{e}_{\boldsymbol{\alpha}}\boldsymbol{\delta t})$ is an indicator function which is equal to zero for fluid and 1 for solid. For both fluids, the value of G_{ads} is equaled with multi-signed which is negative for hydrophilic fluid and positive for lipophilic fluid. A force is applied to fluid due to channel acceleration, as:

$$\mathbf{F}_3 = \rho(\mathbf{x})\mathbf{a} \tag{12}$$

All of these forces such as fluid–fluid force (F_1), fluid–solid force (F_2), and a force due to fluid motion inside the channel applied as the Reynolds number and F_3 which is applied in the equilibrium velocity term, are as follows:

$$\boldsymbol{u}^{\boldsymbol{eq}} = \boldsymbol{u} + \frac{\boldsymbol{\tau}\boldsymbol{F}_{\boldsymbol{total}}}{\boldsymbol{\rho}(\boldsymbol{x})} \tag{13}$$

where, F_{total} is as.$F_{total} = F_1 + F_2 + F_3$[3].

Single-phase thermal LBM

Single-phase thermal LBM is defined by applying a neutral scalar model. In a thermal system, if the effects of viscosity and thermal pressure are not considerable, in the neutral scalar method, the temperature domain is presented as follows [18]:

$$\frac{\partial\mathbf{T}}{\partial\mathbf{T}} + \boldsymbol{u}.\nabla\boldsymbol{T} = \nabla.(\boldsymbol{\kappa}\nabla\boldsymbol{T}) \tag{14}$$

where $\boldsymbol{\kappa}$ and u are the thermal dissipation coefficient and total fluid velocity, respectively. In the neutral scalar method, according to the neutral nature of the temperature domain, similar to the density, one distribution function is proposed for temperature as follows:

$$\mathbf{g}_{\alpha}(\mathbf{x}+\mathbf{e}_{\alpha}\delta\mathbf{t},\mathbf{t}+\delta\mathbf{t}) = \mathbf{g}_{\alpha}(\mathbf{x},\mathbf{t}) - \frac{1}{\tau_{\mathbf{T}}}[\mathbf{g}_{\alpha}(\mathbf{x},\mathbf{t}) - \mathbf{g}_{\alpha}^{\mathbf{eq}}(\mathbf{x},\mathbf{t})] \tag{15}$$

where $\boldsymbol{\tau}_T$ is known as the relaxation time for temperature. The equilibrium distribution function for temperature is defined as:

$$\mathbf{g}_{\alpha}^{\mathbf{eq}} = \omega_{\alpha}\mathbf{T}[1 + 3\mathbf{e}_{\alpha}.\mathbf{u} + \frac{9(\mathbf{e}_{\alpha}.\mathbf{u})^2}{2} - \frac{\mathbf{u}^2}{2}] \tag{16}$$

Similar to density, the temperature is obtained by summing all of the distribution functions, as:

$$\mathbf{T} = \sum_{\alpha=0}\mathbf{g}_{\alpha} \tag{17}$$

Where,$\boldsymbol{\kappa} = \left(\boldsymbol{\tau}_T - \frac{1}{2}\right)\boldsymbol{c}_s^2\boldsymbol{\delta t}$, hence, the Prandtl number can be defined as follows:

$$\mathbf{Pr} = \frac{\mathbf{v}}{\kappa} = \frac{2\boldsymbol{\tau}_{\boldsymbol{v}} - 1}{2\boldsymbol{\tau}_{\boldsymbol{T}} - 1} \tag{18}$$

By changing $\boldsymbol{\tau}_{\boldsymbol{v}}$ or $\boldsymbol{\tau}_{\boldsymbol{T}}$, it can be created with different Prandtl numbers.

Two non-dimensional numbers of Prandtl and Rayleigh numbers are used for describing the states of the system which Prandtl number is obtained from Equation (18) and the Rayleigh number is defined as follows:

$$\mathbf{Ra} = \frac{\mathbf{g}\beta\Delta\mathbf{T}\mathbf{H}^3}{\nu\kappa} \tag{19}$$

Where, g, β, and H are the gravitational acceleration, thermal expansion coefficient, and the grid size along the y-direction. Boussinesq approximation was applied for two-phase RB convection [4]. In this paper, the Boussinesq approximation is applied which assumes that density is proposed to be constant in the consistency equation, except in the term of buoyancy force which density varies linearly with temperature.

$$\rho\mathbf{G} = \rho\beta\mathbf{g}(\mathbf{T} - \mathbf{T}_{\mathbf{avg}}) \tag{20}$$

Where g and $\mathbf{T}_{\mathbf{avg}}$ are the buoyancy force in the weight unit and the initial temperature, respectively. This problem is simulated by using a neutral scalar thermal model. In this method, a wall buoyancy condition is applied to the wall.

Multi-phase thermal LBM

In the current work, two-phase thermal flow can be modeled with the combination of equations of the double-distribution function model of thermal LBM and the multi-phase Shun-Chen model. In this model, fluid dynamics are modeled by using the Shan-Chen model while for determining the temperature domain, a further equation of neutral scalar is used and by defining an external force term, it is merged with the multi-phase isothermal method. The term buoyancy force which is due to gravitational force and also, the temperature difference is presented as [18]:

$$\rho(\mathbf{x})\mathbf{G} = \rho(\mathbf{x})\mathbf{g}\left(1 - \frac{\langle\rho\rangle}{\rho(\mathbf{x})}\right) - \beta\rho\mathbf{g}(\mathbf{T} - \mathbf{T}_0) \tag{21}$$

where $\langle\rho\rangle$ is average density in all of the fluid regions, g is gravitational acceleration, T_0 is the reference temperature whose value is equal to the temperature of the system in the condition of pure convection and also, β is a fluid thermal expansion which is proposed equal for both fluids. On the left side of Equation (21), the first term shows the buoyancy force caused by density difference, and also, the second term indicates the gravitational force caused by temperature difference. Although this method has a modest concept, it can be applied to the various state equations of an ideal gas and extracted temperature domain. In comparison with the other multi-phase thermal methods, the presented model has a simpler concept and higher stability because there is no demand to augment particle velocity or trace interface. In this method, the stability is computed by fluid dynamics and also, and the temperature domain does not influence it. Capillary and Rayleigh's numbers include all of the impressive parameters except the pressure and contact angle of the surface. These non-dimensional parameters can be computed as follows:

$$Ra = \frac{g\beta\mathrm{H}THPr}{\nu^2},\ Ca = \rho\nu\sqrt{\frac{g\beta\Delta TH}{\sigma}}, Nu_{avg} = 1 + \frac{u_y(T - T_{avg})N_y}{\Delta T} \tag{22}$$

where ρ, g, β and N_y are the density of each fluid, gravitational acceleration, thermal expansion coefficient, and grid size along the y-

Table 1
The value of the average Nusselt number in the various grid sizes for $Ra = 8 \times 10^4$ and..$Ca = 4.6 \times 10^{-4}$

grid size	Nu_{avg}
50×100	2.54
90×180	2.6
150×300	2.62

direction, respectively. In addition, ΔT is the difference between the upper and lower walls ($\Delta T = T_H - T_C = 1$), u_y is the velocity in the y-direction, T* is the fluid temperature in the pure conduction (the reference temperature), N_y is grid size along the y-direction, and all parameters in $\langle\,\rangle$ Represent average flow in all of the regions and σ is surface tension. It should be noted that in this problem, the parameter of $\varepsilon = \beta\Delta T$ has significant importance. For a non-dimensioning time, $t = \sqrt{\frac{H}{g\beta\Delta T}}$ is proposed.

Numerical procedure and assumptions

Grid validation

To ensure the results independency from the grid size, this problem is simulated in different grid sizes and obtained Nusselt numbers are compared with each other. In fluid dynamics, the Nusselt number (Nu) is the ratio of convective to conductive heat transfer in a fluid. Table 1 indicates the computed Nusselt number in different grid sizes for $Ra = 8 \times 10^4$ and $Ca = 4.6 \times 10^{-4}$. The Rayleigh number (Ra) for a fluid is a dimensionless number associated with buoyancy-driven flow, also known as free or natural convection and the capillary number (Ca) is a dimensionless quantity representing the relative effect of viscous drag forces versus surface tension forces acting across an interface between a liquid and a gas, or between two immiscible liquids. As seen, the variation of the Nusselt number is about 2 %. Hence, the time of solving is lower in the larger grids, Also, if the grids become larger than a certain limit, the answers will not be accurate. in the following simulations, a 90×180 grid is used. The average Nusselt number is calculated by $Nu_{avg} = \frac{1}{L}\int \frac{\partial T}{\partial x}$ which the integral is on the hot surface and L is the height of the cavity. Variation of the Nusselt number was taken unidirectional Because heat transfer takes place in the vertical direction and the Nusselt number shows the changes of heat transfer in the horizontal direction well.

Validation

Before studying the effective parameters in the Rayleigh–Bénard phenomenon, validation is performed for the computer program. Fig. 3 compares the temperature domain of the present study with the results of Chang and Alexander [4] for $Ra = 8 \times 10^4$ and $Ca = 4.6 \times 10^{-4}$ and $\varepsilon = 0.15$ in two-time steps ($\varepsilon = \beta\Delta T$). The lattice Boltzmann method (LBM) is extended to include the effects of interfacial tension and its

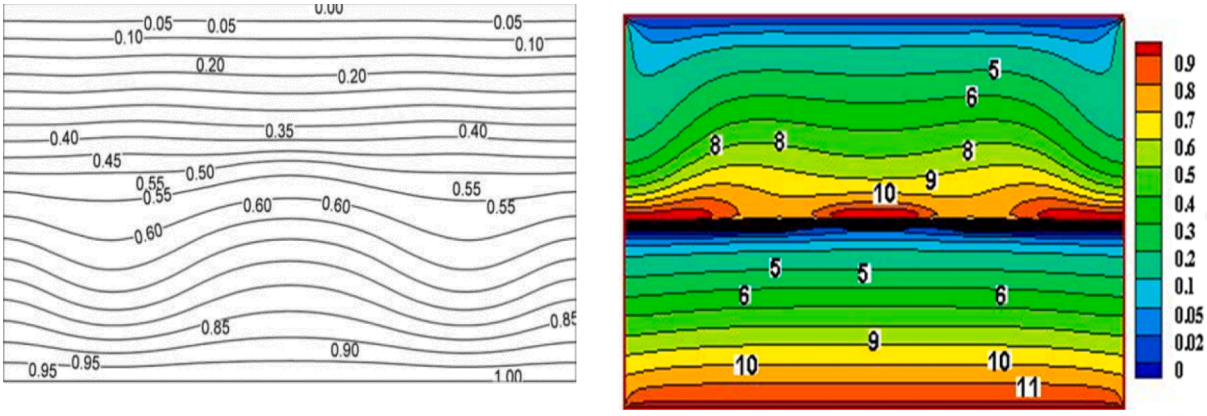

(a) $t = 65$

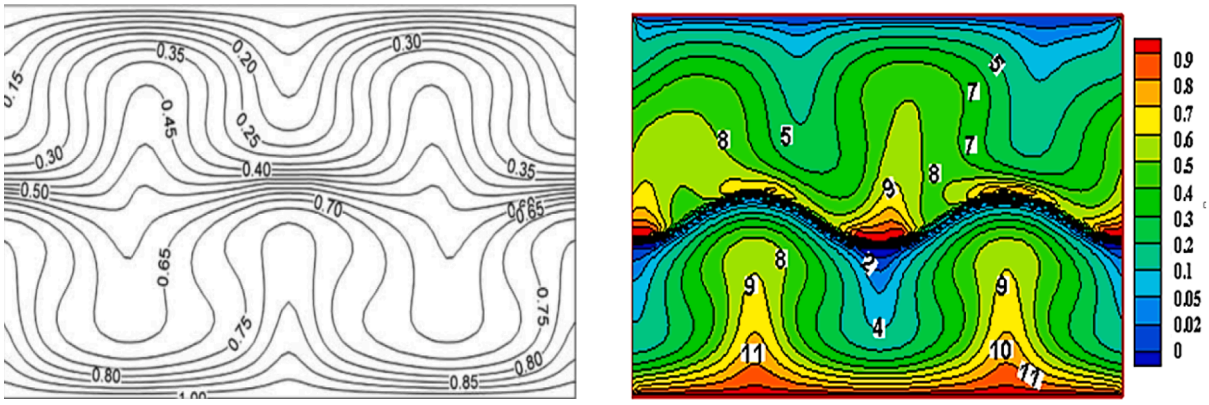

(b). $t = 720$

Fig. 3. Time changes of isothermal lines in the present study (right side) and Chang and Alexander [4] (left side) for..$Ra = 8 \times 10^4, Ca = 4.6 \times 10^{-4}, \varepsilon = 0.15$

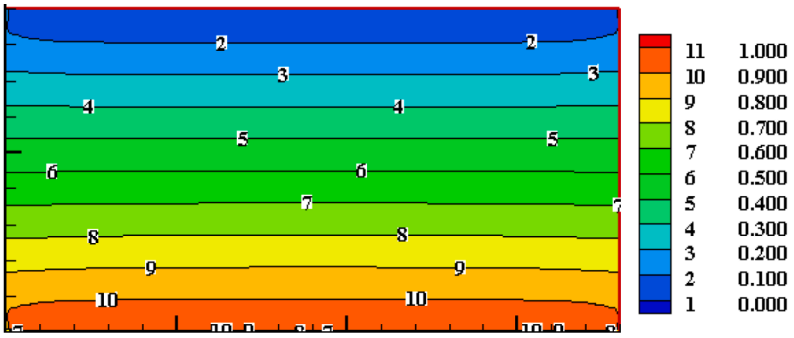

(a). Isothermal lines in $Ra = 10^3$

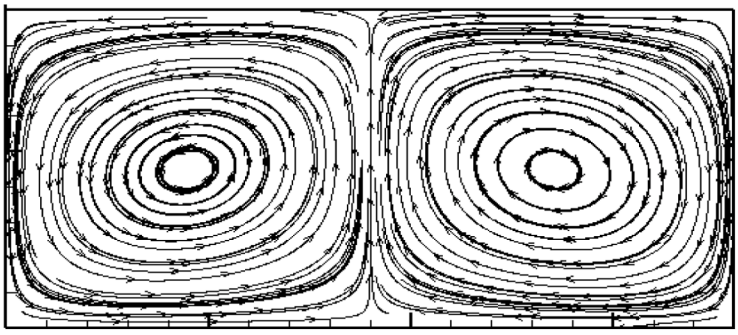

(b). Stream lines in $Ra = 10^4$

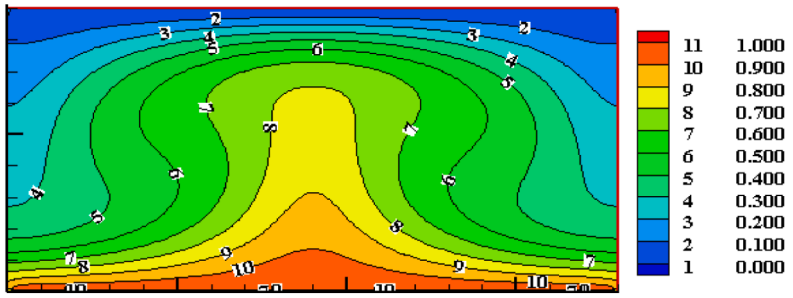

(c). Isothermal lines in $Ra = 10^4$

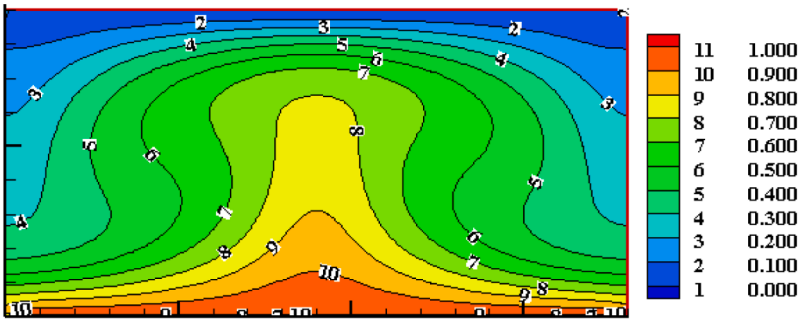

(d). Isothermal lines in $Ra = 10^5$

Fig. 4. Isothermal liens and streamlines for Rayleigh–Bénard problem in different Rayleigh numbers and Pr = 1.

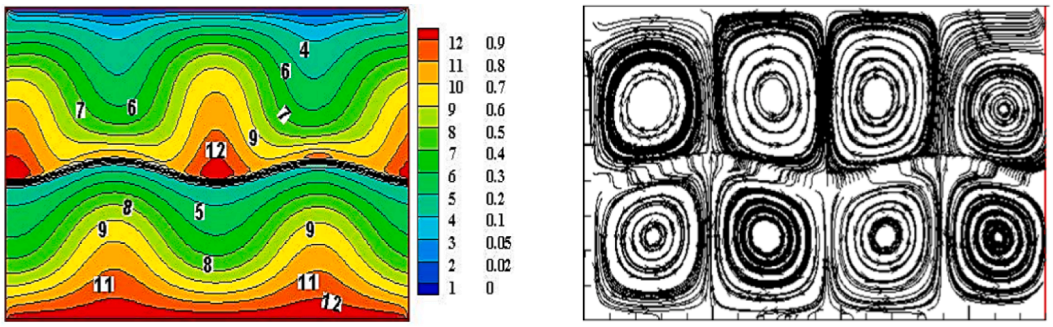

(a). $\boldsymbol{Ra = 1.2\times10^{3}}$

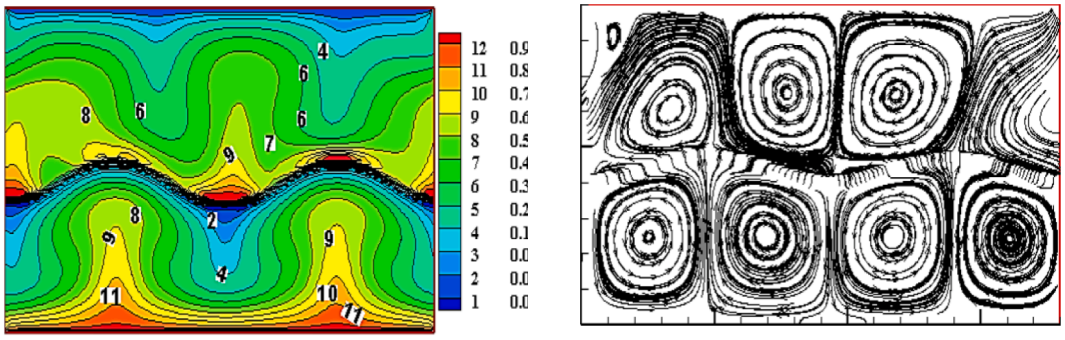

(b). $\boldsymbol{Ra = 8\times10^{4}}$

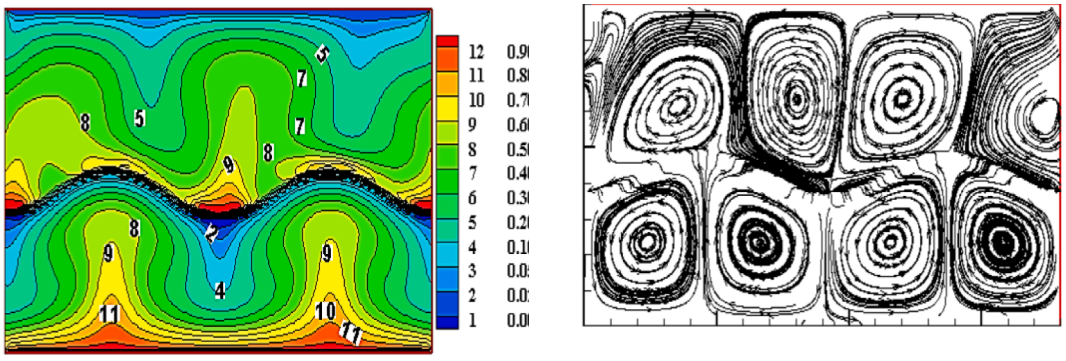

(c). $\boldsymbol{Ra = 2\times10^{5}}$

Fig. 5. Isothermal lines (left side) and streamlines (right side) for $Ca = 4.6 \times 10^{-4}, \varepsilon = 0.15$ and different Rayleigh numbers.

temperature dependence and is applied to the problem of buoyancy-driven flow in a nonisothermal two-phase system. No prior assumptions are made regarding the shape and dynamic roles of the interface. The behavior of the interface is obtained as part of the solution of the lattice Boltzmann equations. A parametric study of the effects of thermally induced density change, buoyancy, and surface tension variation with temperature on interface dynamics, flow regimes, and heat transfer is presented.

As seen, by enhancing the number of time steps time step,(In all these studies, time is dimensionless and it means the number of steps.) the interface between two fluids changes, and convective heat transfer becomes complete. In addition, since this work is transient, there is a proper agreement between the two works. The only difference is that in this paper because of high spurious current, the temperature rises abnormally at the boundary of two fluids. Spurious current is one of the defects of the used method that causes errors in the results. This effect can be reduced by using modified methods. One of the disadvantages of the present study is that the effects of false velocities at the fluid boundary are significant and can cause many changes. These two studies should be compared qualitatively with each other because different equations were used and the origin of time steps in the two studies are different from each other. The two studies, are very similar in terms of increasing the number of time steps time step, the heat transfer becomes more complete and reaches a stable state. In Figs. 1-a, Rayleigh–Bénard heat transfer has not occurred completely and in the isothermal lines, there are fewer ascending and descending. As seen, in both works, there is lower Rayleigh–Bénard heat transfer in the fluid with low density (upper fluid). If the density of two fluids is equal, the problem will be similar to the Rayleigh-Bernard single phase. Since, heat transfer is the time needed, as time passes, Rayleigh–Bénard convective heat transfer occurs and the ascending and descending of isothermal lines become more regular. When conductive heat transfer flow is started, the random

motions start in the microscopic scale automatically. After these effects appear on the macroscopic scale, fluid formation occurs as the Bénard convective cells. The period of Bénard cells will continue as stable until there is a constant temperature difference between the two plates. This period alternates from clockwise to counterclockwise in the x-direction. It is worth mentioning that the variations of surface tension are not calculated because, in the Shan-Chen model, the surface tension is obtained from the Laplace test and cannot be changed directly.

Results and discussion

Results for single-phase Rayleigh–Bénard

Fig. 4 shows Rayleigh–Bénard convection for different Rayleigh numbers in Pr = 1. When the value of the Rayleigh number is low, the heat transfer only occurs as the conductive heat transfer and temperature distribution show pure conduction according to Figs. 4-a. In this figure, only thermal conduction occurs and there is no convective flow. However, when the Rayleigh number is greater than the critical Rayleigh number, each small turbulence causes the start of the convective heat transfer. Figs. 4-b indicates the flow domain in convective heat transfer. As seen these lines are completely symmetric and convective flow in the Rayleigh–Bénard convection is illustrated in a good way. According to Figs. 4-c, by developing flow, it finally system reaches a stable state with the specified temperature distribution and as seen in Figs. 4-d, the temperature in the wall increases, but its value is not noticeable and is not specified in the figure. For this two-dimensional horizontal channel which is influenced by periodic boundary conditions from the walls, the value of the critical Rayleigh number is equal to $Ra_c = 1708$ by linear stability theory.

When the Rayleigh number becomes greater than the critical Rayleigh number, in addition to conductive heat transfer, convective heat transfer also occurs. According to that convective heat transfer is dominated, due to this phenomenon, the fluid assumes a regular and specified shape similar to the hexagonal cell which in fluid dynamics science and related phenomenon to the convective cells is called Bénard cells.

Results for Rayleigh–Bénard heat transfer in a two-phase system

Two-phase Rayleigh–Bénard

Rayleigh–Bénard convective heat transfer is extensively used in the industry where here this problem is described with the aid of LBM. In the previous section, this problem is presented as a single phase. Here, two immiscible fluids with different temperatures are considered between two isothermal solid plates. A two-layer system of immiscible fluids with an equal thickness of $\boldsymbol{h_1} = \boldsymbol{h_2} = 0.5\boldsymbol{H}$, the width of W and height of H. The ratio of densities is equal to $\boldsymbol{\rho_r} = 0.33$.

The effect of the changes in Rayleigh number

Fig. 5 shows the variations of streamlines and isothermal lines in $\rho_r = 0.33$**and** $\boldsymbol{Ca} = 4.6 \times 10^{-4}$ for the various Rayleigh numbers. It is worth mentioning that 10^5 is considered a high Rayleigh number [14]. By incrementing the Rayleigh number from 1.2×10^3 to 8×10^4, the variations of the amplitude of interface augment, however by enhancing Rayleigh number from 8×10^4 to 2×10^5, the interface is almost unchanged. The parameter range used is due to the possibility of validation with the reference article and the fact that the equations are responsible in a certain range.

By augmenting the Rayleigh number, the temperature gradient increases in the vicinity of the upper wall, lower wall, and interface. According to this figure, in the upper fluid which has a lower density, flow domain circulation is weaker this subject shows that by increasing density, heat transfer augments. According to $\frac{\Delta h}{H}$ parameter, by changing the Rayleigh number, the variations of the interface are not influenced

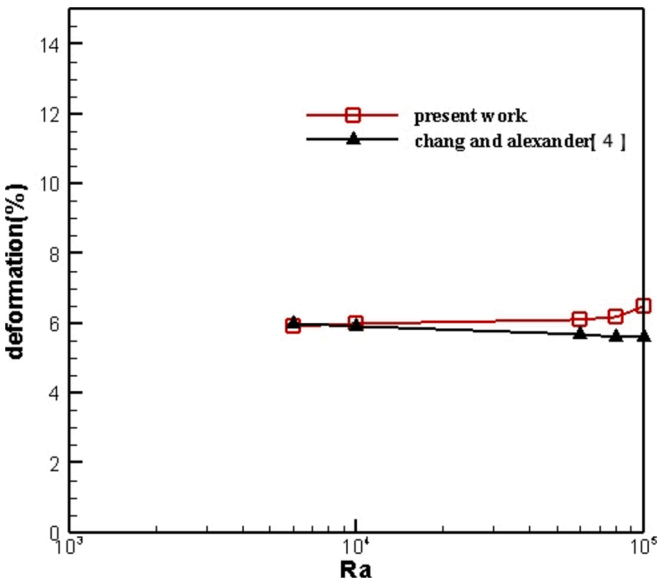

Fig. 6. The variations of interface for each Rayleigh number in..$Ca = 4.6 \times 10^{-4}$and $\varepsilon = 0.1$

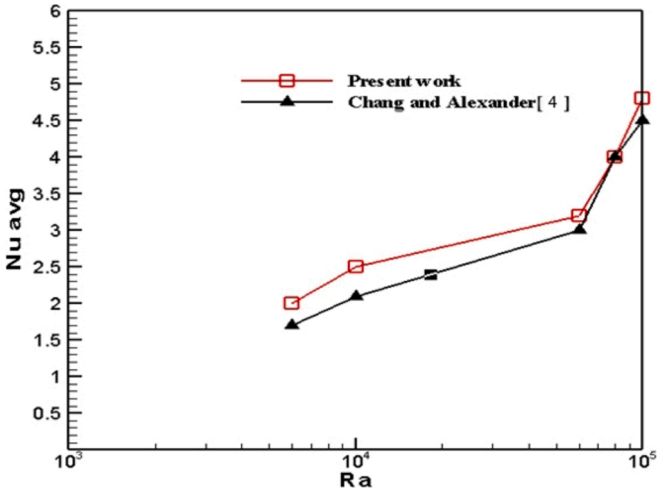

Fig. 7. The variations of average Nusselt number for each Rayleigh number in..$Ca = 4.6 \times 10^{-4}$and $\varepsilon = 0.15$

significantly. Fig. 6 indicts the variations of interface for each Rayleigh number in $Ca = 4.6 \times 10^{-4}$and $\varepsilon = 0.1$. It can be concluded that the variations of interface change insignificantly by increasing Rayleigh numbers. In addition, in this figure, the results of the present study are compared with the results of Chang and Alexander [4]. The insignificant difference in the graph is due to the different solving methods of the two types of research. It should be noted that two works have used different methods to solve the problem and this has caused differences in the diagrams. The emergence of spurious currents has made the problem problematic. Also, in this work, we are trying to measure the ability of the two-phase Boltzmann network method, which can be improved with the modified model. Fig. 7 illustrates the average Nusselt number for each Rayleigh number for $Ca = 4.6 \times 10^{-4}$and $\varepsilon = 0.15$. The average Nusselt number increases by augmenting the Rayleigh number indicating that Rayleigh–Bénard heat transfer increments by incrementing the Rayleigh number. Fig. 7 compares the average Nussle number with the results of Chang and Alexander [4] in different Rayleigh numbers which indicate good agreement. According to the last results in Fig. 5, by increasing the Ra number, the temperature gradient near the walls

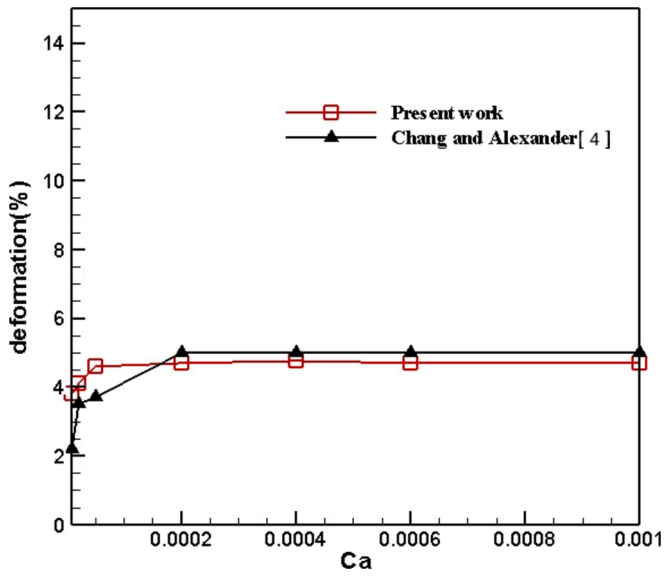

Fig. 8. The changes of interface for each Capillary number in..$Ra = 8 \times 10^4$ and$\varepsilon = 0.15$

increases which causes the Nu number increment. Thus, Nu growth is a result of a temperature gradient in the vicinity of walls.

The effect of changes in Capillary number

The effect of changes in Capillary number on the changes in the interface is illustrated in Fig. 8 in $Ra = 8 \times 10^4$ and $\varepsilon = 0.15$ which the changes of surface tension with temperature are neglected. As seen, in lower Capillary numbers, the changes of interface enhance up to 4.2 %, after that by incrementing Capillary number, the variations of the interface are almost unchanged. In this figure, the present results are compared with the results of Chang and Alexander [4]. As seen, in a Capillary number of less than 2×10^{-4}, the results of Chang and Alexander [4] have a small difference from the results of this paper. However, in higher Rayleigh numbers, appropriate concordance is seen. The reason for this small difference is because of different simulation methods.

The effect of variation of ε parameter

In this section, the effect of variation of $\varepsilon = \beta \Delta T$ parameter is investigated. According to Fig. 9, by increasing ε, the variations of the interface are enhanced. Consequently, the variations of the interface are changed only by changing the thermal expansion coefficient and the temperature difference between the two walls. When the value of ε is too high, the variations of the interface cannot be neglected. Fig. 10 represents the variations of interface with the ε parameter in $Ra = 8 \times 10^4$and $Ca = 4.6 \times 10^{-4}$. As seen, in Fig. 10 the deformation of the interface augments by increasing ε. When $\varepsilon \leq 0.1$, the rate of deformation is less than 3 % which can be neglected. However, for higher ε, the

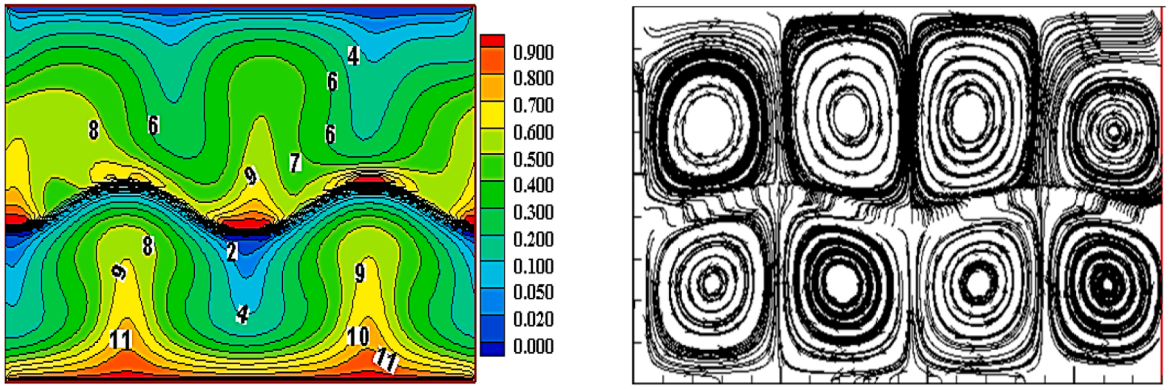

(a). ε = 0.1

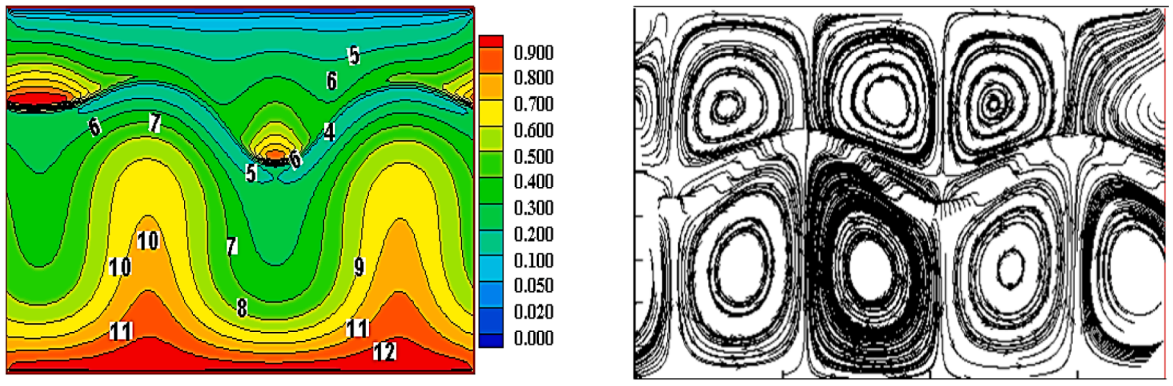

(b). ε = 0.3

Fig. 9. Isothermal lines (left side) and streamlines (right side) in different ε in..Ra $= 8 \times 10^4$and Ca $= 4.6 \times 10^{-4}$

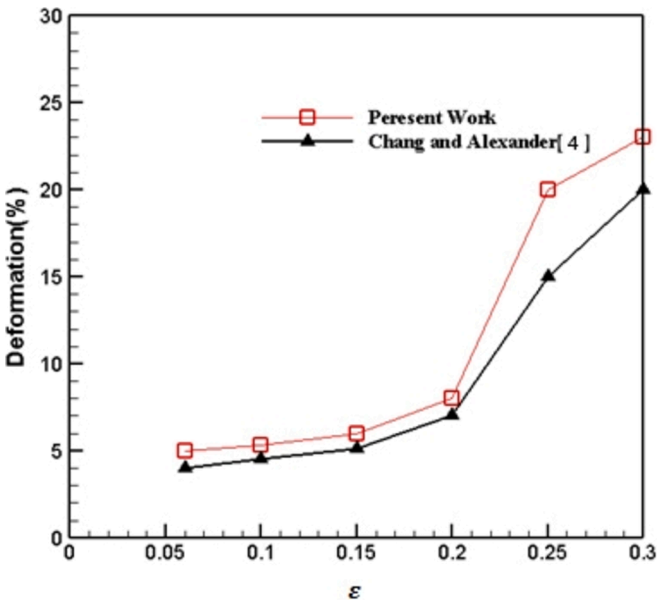

Fig. 10. Variations of fluids interface for each ε in..$Ra = 8 \times 10^4$and$Ca = 4.6 \times 10^{-4}$

variations of the interface cannot be neglected. If the density of two fluids is not equal, the range will change. In general, in the high time step, the amplitude will change and these changes are related to the characteristic length.

Conclusion

In the current work, a multi-phase thermal model of LBM is described. In this model, by using the Shan-Chen model of LBM and the neutral scalar model of LBM, fluid mechanics, and temperature domain are simulated, respectively. The multi-phase thermal model of LBM is presented from the combination of the single-phase thermal model and the multi-phase isothermal model of LBM. For instance, the single-phase Rayleigh–Bénard problem and the effects of the Rayleigh number are studied on heat transfer. In Rayleigh–Bénard convection heat transfer, if the Rayleigh number is greater than the critical Rayleigh number, it causes instability in the flow domain which leads to creating convective heat transfer. By augmenting the Rayleigh number, the rate of heat transfer is enhanced. In the following, two-phase Rayleigh–Bénard convective heat transfer is analyzed in different Rayleigh and Capillary numbers and also, at different times. In the two-phase Rayleigh–Bénard problem, by enhancing the Rayleigh number, the temperature gradient increases in the vicinity of upper and lower walls and interface, and also, the power of flow domain circulation becomes weaker. At high Rayleigh numbers, the influence of spurious currents increases, which affects the accuracy of the results. The variations of the interface are not considerably influenced by changing the Rayleigh number according to $\frac{\Delta h}{H}$ parameter. In lower Capillary numbers, the changes of interface augment up to 4.2 % then by increasing Capillary number; the variations of the interface are almost constant. In Rayleigh–Bénard, the variations of the interface are changed only by changing the thermal expansion coefficient and temperature difference between the two walls. By augmenting ε, the deformation of the interface increases. If $\varepsilon \leq 0.1$, the rate of deformation is less than 3 % this small ratio is negligible, however for higher ε, the changes in the interface cannot be neglected. As can be seen in all the shapes and descriptions, the changes in the shape of the common surface have the greatest effect on the parameter ε. Moreover, employing the Shan-Chen model for simulation of the common surface of multi-phase flow prepares needless conditions to calculate surface tension in numerical commutations. In future research, the effects of spurious current can be reduced by using the modified Shan-Chen model to make the answers more realistic. It is also possible to simulate problems in which phase change occurs. The results indicate that in multi-phase problems the presence of temperature as an obstacle, delays reaching the stable state.

Declaration of competing interest

The authors declare that they have no known competing financial interests or personal relationships that could have appeared to influence the work reported in this paper.

Data availability

No data was used for the research described in the article.

References

[1] X. He, S. Chen, G.D. Doolen, A novel thermal model for the lattice Boltzmann method in the incompressible limit, J. Comput. Phys. 146 (1998) 282–300.
[2] R. Zhan, H. Chen, Dynamics of rising CO_2 bubble plumes in the QICS field experiment: Part 2–Modelling, Int. J. Greenhouse Gas Control (2002).
[3] P. Yuan, L. Schaefer, A thermal lattice Boltzmann two-phase flow model and its application to heat transfer problemsdPart 2. Integration and validation, J. Fluids Eng. 128 (2006) 151–156.
[4] Q. Chang, and J. I. D Alexander., "Application of the lattice Boltzmann method to two-phase Rayleigh–Bénard convection with a deformable interface." Journal of Computational Physics, vol. 212, pp. 473-489, 2006.
[5] Z. Dong, W. Li, Y. Song, A numerical investigation of bubble growth on and departure from a superheated wall by lattice Boltzmann method, International Journal Heat and Mass Transfer 53 (2010) 4908–4916.
[6] E. Attar, C. Korner, Lattice Boltzmann model for thermal free surface flows with liquid-solid phase transition, International Journal Heat and Fluid Flow. 32 (2011) 156–163.
[7] S. Chen, K.H. Luo, C. Zheng, A simple enthalpy-based lattice Boltzmann scheme for complicated thermal systems, J. Comput. Phys. 231 (1) (2012) 8278–8294.
[8] M. Ikeda, A novel multi-phase multi-component thermal lattice boltzzman model, J. Comput. Phys. 200 (2012) 153–176.
[9] S. Gong, P. Cheng, Lattice Boltzmann simulation of periodic bubble nucleation, growth and departure from a heated surface in pool boiling, International Journal Heat and Mass Transfer 53 (2013) 123–132.
[10] M. R. Kamali, J. J. J.Gillissen, and H. A. Akker," Lattice-Boltzmann-based two-phase thermal model for simulating phase change," Physical Review E, vol. 88, pp. 267-275, 2013.
[11] M. Taghilou, M.H. Rahimian, Lattice Boltzmann model for thermal behavior of a droplet on the solid surface, Int. J. Therm. Sci. 86 (2014) 1–11.
[12] T. Lee, Effects of incompressibility on the elimination of parasitic currents in the lattice Boltzmann equation method for binary fluids, Computational Mathematic. 58 (2009) 987–989.
[13] Q. Li, Q. J. Kang, M. M. Francois, Y. L. He, and Luo K. H.,"Lattice Boltzmann modeling of boilingheat transfer: The boiling curve and the effects of wettability," International Journal of Heat and Mass Transfer,vol. 85, pp. 787-796, 2015.
[14] X. Shan, H. Chen, Lattice Boltzmann model for simulating flows with multiple phases and components, Phys. Rev. E 47 (1993) 1815–1819.
[15] Kh. Hosseinzadeh · So. Roghani · A. R. Mogharrebi · A. Asadi · D. D. Ganji, "Optimization of hybrid nanoparticles with mixture fluid flow in an octagonal porous medium by effect of radiation and magnetic field", Thermal Analysis and Calorimetry.2020, s10973-020-10376-9.
[16] A. K. Rostami, Kh. Hosseinzadeh & D. D. Ganji, "Hydrothermal analysis of ethylene glycol nanofluid in a porous enclosure with complex snowflake shaped inner wall", Waves in Random and Complex Media.2020, 1745-5030 (Print) 1745-5049.
[17] Kh. Hosseinzadeh, So. Roghani, A. R. Mogharrebi, A. Asadi & D. D. Ganji, "Hydrothermal analysis of ethylene glycol nanofluid in a porous enclosure with complex snowflake shaped inner wall", Journal of Thermal Analysis and Calorimetry volume 143, pages1413–1424(2021),2020.
[18] A.o. Xu, W. Shyy, T. Zhao, Lattice Boltzmann modeling of transport phenomena in fuel cells and flow batteries, Acta Mech. Sin. 33 (2017), https://doi.org/10.1007/s10409-017-0667-6.